The Damping and Flame-Retardant Properties of Poly(vinyl chloride)/ Chlorinated Butyl Rubber Multilayered Composites

Fengshun Zhang, Guansong He, Kangming Xu, Hong Wu, Shaoyun Guo
Polymer Research Institute of Sichuan University, State Key Laboratory of Polymer Materials Engineering, Chengdu,, People's Republic of China
Correspondence to: H. Wu (E-mail: wh@scu.edu.cn) and S. Guo (E-mail: nic7702@scu.edu.cn)

ABSTRACT: The alternating multilayered damping composites, which were consisted of chlorinated butyl rubber (CIIR) layers and poly(vinyl chloride) (PVC) layers, were first prepared through multilayered coextrusion technology. The multilayered structure was controlled by adjusting the layer number or the thickness ratio of CIIR layer and PVC layer. The damping and flame-retardant properties of the CIIR/PVC multilayered damping composites were investigated by dynamic mechanical analysis, the limiting oxygen index, and thermogravimetric analyzer, respectively. The results showed that the effective damping temperature range was broadened with increasing the layer number, since multilayered structure resulted in partial overlap of the loss peaks of CIIR and PVC. Meanwhile, the flame-retardant properties of the multilayered composites were also enhanced with increasing the layer number. Less surface area of CIIR contacting oxygen in the confined burning space, rather than the formation of char residue, could effectively retard the combustion of the material. © 2014 Wiley Periodicals, Inc. J. Appl. Polym. Sci. **2015**, *132*, 41259.

INTRODUCTION

Viscoelastic polymers have been widely used as damping materials to reduce the vibration and noise in transportation, civil construction, precision instrument, and military equipment, due to their outstanding properties for reducing vibration and noise around the glass transition temperature (T_g).[1,2] The chlorinated butyl rubber (CIIR), halogenated derivative of butyl rubber, is well-known for its excellent capability of energy dissipating combining with good air tightness, ozone resistance, and chemical stability.[3] However, the drawbacks of CIIR such as flammability in the air and its loss peak below room temperature, result in the loss of life and property and poor damping property at room temperature.[4] Therefore, CIIR used as damping material is often limited.

Many efforts have been devoted to extend the damping functional region of CIIR toward high temperature area.[4–6] Blending and interpenetrating network with high T_g polymer have been used to improve the damping property of CIIR at room temperature. For example, Wu and coworkers[5] have found that the CIIR/petroleum resins blends only show a single loss peak, and the height of the loss peak increases and the peak location shifts to high temperature with increasing the content of petroleum resins. Moreover, Liao and coworkers[6] have prepared a series of dynamically cured butyl rubber/polypropylene blends, loss peaks of the blends tend to shift toward high temperature. But the tan δ_{max} is not over 0.35, since the maximum of loss peak is suppressed due to the addition of polypropylene.

Conversely, flame-retardant property of the damping composite is very important, especially for aerospace, railway, and maritime fields,[7] where the damping materials are most often used. Unfortunately, flame-retardant property of the CIIR is not satisfying, because its limiting oxygen index (LOI) is only about 21. Meanwhile, according to the experimental work of our laboratory, the CIIR/petroleum resins composites, whose LOI is even below 19, become more flammable.[8] Though it might be advantageous to improve the flame-retardant property of CIIR by blending with inorganic fillers such as organophilic montmorillonite, the damping peak would decrease significantly and move to low temperature.[9] Therefore, it seems difficult to acquire high damping property and good flame-retardant property simultaneously. Little literature is focused on the combination of damping and flame-retardant properties.

Researchers have blended acrylic rubber[10] and nitrile rubber[11] with poly(vinyl chloride) (PVC) to broaden the effective damping temperature range, especially for the damping property above room temperature. Moreover, PVC has good flame-retardant properties due to its high chloride content.[12] In our opinions, the addition of PVC should improve damping and

flame-retardant property simultaneously. Furthermore, there is appropriate intermolecular interaction between PVC and CIIR with a chlorination concentration of 1.2%, which is exactly required for excellent damping materials.[13]

In our previous work, multilayered structure is proposed as an optimal route to fabricate flame-retardant composites with excellent mechanical properties.[14] In addition, there is a new intermediate damping peak in the multilayered composite, which becomes dominant with increasing the layer number, indicating that the effective damping temperature range (Tan $\delta_{max}>0.3$) can be broadened.[15] In this work, the multilayered damping composites, consisting of CIIR layers and PVC layers, have been first prepared through multilayered coextrusion. The multilayered structure is controlled by adjusting the layer number or the thickness ratio of CIIR and PVC layers. The damping and flame-retardant properties of the composites are characterized by dynamic mechanical analysis (DMA), the LOI, and thermogravimetric analyzer (TGA), respectively.

EXPERIMENTAL

Materials and Specimen Preparation

The CIIR (product code: CBK 139) with a chlorination concentration of 1.2% was from Nizhnekamsk (Russia). A laboratory-scale mixer equipped with a pair of roller blades was used for blending CIIR with 40 phr (parts per hundred parts of resin) carbon black, 10 phr white oil and 1 phr stearic acid via mechanical mixing at room temperature for 8 min.

The PVC resin used in this work was a commercial suspension grade with degree of polymerization of 1100–1000 (SG-5, Sichuan Jinlu Group Co., Deyang, China). In a high speed mixer, the PVC was mixed with 2 phr organotin stabilizer, 0.5 phr stearic acid, and 100 phr chlorinated paraffin. The carbon black, white oil, organotin stabilizer, stearic acid, and chlorinated paraffin were commercial products.

The multilayered damping composites were coextruded as a sheet about 2 mm thick and 40 mm wide through the multilayered coextrusion system designed by our lab, as described previously.[16,17] In this work, 2, 8, and 32 layers samples were extruded with 0, 2, and 4 layer multiplying elements (LMEs), respectively. The ratio of two components was varied by adjusting the screw speed of extruders. The temperatures of extruders for PVC and CIIR were 140°C and 130°C, respectively, and the temperature of LMEs was 140°C.

For comparison with multilayered composites, conventionally blended CIIR/PVC samples were prepared. At first, to disrupt the alternating multilayered structure, the multilayered composites were kneaded by tow-mill for 8 min at 140°C. Furthermore, the conventional CIIR/PVC blends were hot compressed to form 2-mm-thick sheets for testing.

To investigate the effect of layered structure on the damping property, the orientation and the thermal history caused by processing would be eliminated by heat treatment. The multilayered and conventionally blended CIIR/PVC composites were maintained at 140°C for 10 min, and then cooled to room temperature. At the temperature of 140°C, the orientation
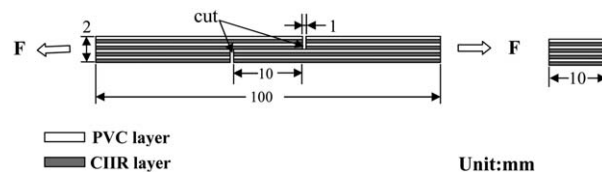

Figure 1. The schematic of the 8-layer composite for lap shear measurement.

structures of CIIR and PVC molecular chains could melt and be eliminated.

Morphological Observation

A scanning electron microscopy (SEM, JSM-5900LV, Japan) was used to study the morphology of the conventionally blends and multilayered composites. All the samples were quenched in liquid nitrogen for 1 h and then were cryogenically fractured. The fractured section was parallel to extrusion direction and perpendicular to surface of multilayered composites. To observe the CIIR morphology more clearly, the fractured sections of conventional blends were etched with hexane for 10 min to extract CIIR phase preferentially. Before testing, these samples were sputter coated with Au.

Dynamic Mechanical Analysis

In this work, the DMA was acquired through a dynamic mechanical analyzer (Q800, TA Instrument). The samples with sizes of 30 mm (length), 10 mm (width), 2 mm (thickness) were heated from $-70°C$ to $80°C$ at a heating rate of $3°C/min$ under single cantilever bending mode and the testing frequency was 10 Hz. The direction of dynamic load was perpendicular to the interfaces.

Measurement of Interfacial Adhesion Strength

Interfacial adhesion strength of the specimens was characterized by lap shear test. All the multilayered specimens were cut in a lap shear joint geometry, for example, the schematic of the 8-layer composite for lap shear measurement was shown in Figure 1. Stress–strain behaviors were measured with an Instron 5567 machine (Canton, MA) operating in tension mode at $23 \pm 2°C$. A crosshead speed of 50 mm/min was used in the test. The shear strength was calculated as the maximal load divided by lap area of shear plane. At least of five specimens for each sample were tested and the average value was calculated.

Burning Experiments

The LOI values were measured by an oxygen index meter (HC-2C, Jiangning Analytical Instrument Factory, China). The dimensions of each specimen are $130 \times 6.5 \times 1.5$ mm^3. The direction of combustion measurement was parallel to the interfaces of the multilayered specimen.

Thermogravimetric Analyzer

All thermogravimetric tests were performed on a TGA (TG-209F1, NETZSCH, Germany). Each sample, with a weight of 5–10 mg, was heated from $30°C$ to $700°C$ at a rate of $10°C/min$ in air.

Density Measurement

The densities of the samples were tested in a GH-120M high precision density tester (Matsuhaku, Taiwan), the measuring
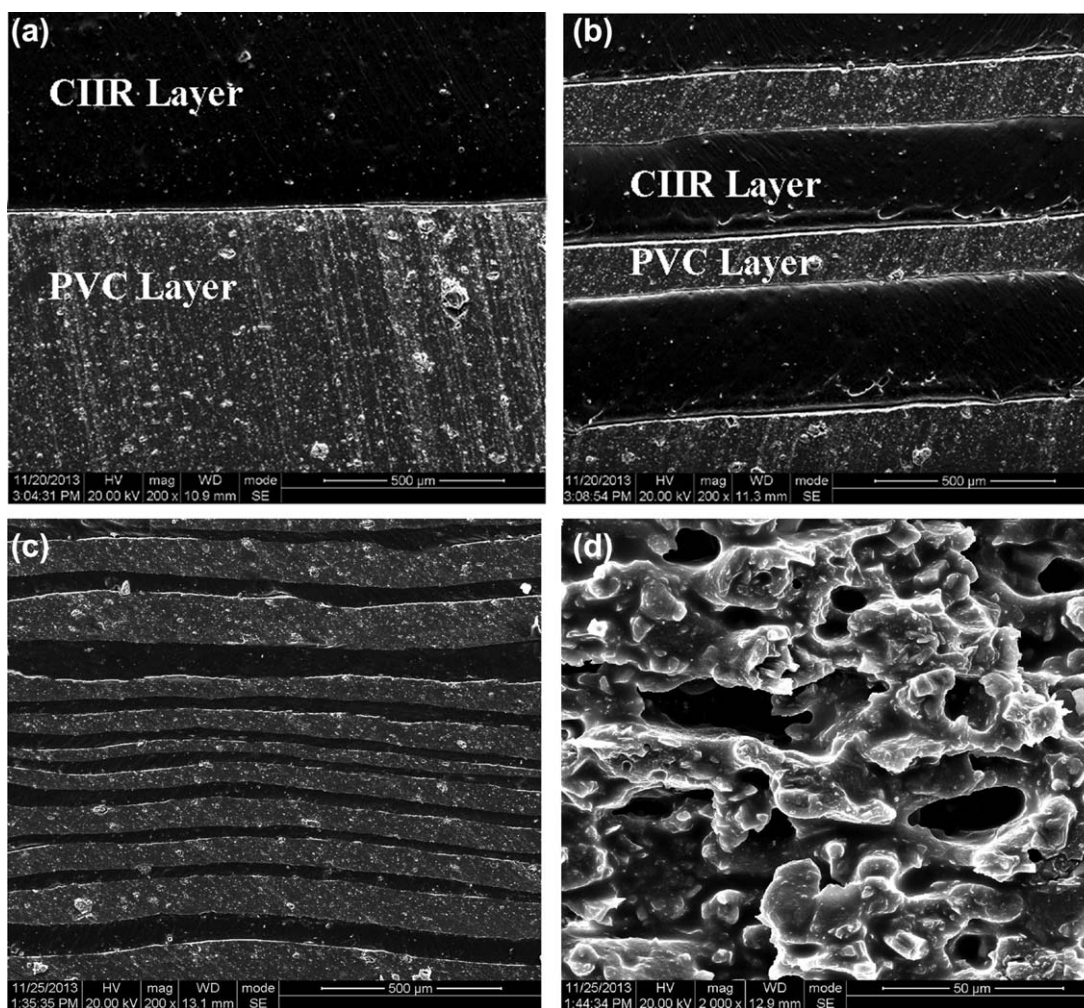
Figure 2. The SEM images of (a) 2- layer, (b) 8- layer, (c) 32-layer, and (d) conventional blended CIIR/PVC composites.

accuracy of which was 0.1 kg/m^3. The measured densities of the CIIR and PVC were 0.9212×10^3 and 1.3771×10^3 kg/m^3, respectively. According to the measured density of the composite, the volume fraction of the PVC (V_{PVC}) could be found using the following equation:

$$V_{PVC} = \frac{\rho_C - \rho_{CIIR}}{\rho_{PVC} - \rho_{CIIR}}$$

ρ_C is the density of the composite, ρ_{CIIR} is the density of CIIR, ρ_{PVC} is the density of PVC.

RESULTS AND DISCUSSION

Phase Morphology

Figure 2 shows SEM micrographs of multilayered [Figure 2 (a–c)] and conventional blend [Figure 2(d)] CIIR/PVC damping composites with the 3:2 screw speed of extruders. It is illustrated that the blend composite has typical sea-island morphology because of the partial miscibility between PVC and CIIR, and the CIIR phases are evenly distributed in the PVC matrix. Conversely, the multilayered samples show a special co-continuous layered morphology, which can not be achieved through general processing methods. From the SEM micrographs, with the layer number

increasing, the thickness of CIIR layers and PVC layers decrease significantly. The volume fractions of the CIIR and PVC that are acquired by the density measurement method are listed in Table I. It is clear that, for the conventional blend and the multilayered specimens with the same extruding ratio, the volume fractions of the CIIR and PVC do not change distinctly with the number of layers changing. The content (or layer thickness) ratio of two components is varied by adjusting the screw speed of extruders.

Dynamic Mechanical Properties of CIIR and PVC

Figure 3(a) shows the dynamic mechanical properties of CIIR and PVC versus temperature, respectively. As first discovered by Ferry and coworkers,[18] the tan δ curve of CIIR reveals an asymmetrical double-peak structure with a maximum on the high temperature side and an additional shoulder on the other side. The loss peak of CIIR is pretty wide covering a temperature range from $-47°C$ to $28°C$ (tan $\delta > 0.3$) with a maximum at $-15°C$ and a shoulder peak near $-37°C$. Among it, the shoulder and the maximum are the reflections of different relaxation processes with different motion scales. The low-temperature shoulder peak corresponds to the T_g of CIIR; while

Table I. The Content of the CIIR and PVC in the Composites

Sample code	Extruding rate (r/min)		Density ($\times 10^3$ kg/m^3)	Volume fraction of CIIR (%)	Volume fraction of PVC (%)
	CIIR	PVC			
CIIR	–	–	0.9212	100	–
PVC	–	–	1.3771	–	100
2L 3 : 2	300	200	1.1669	46.1	53.9
8L 3 : 2	300	200	1.1719	45.1	54.9
32L 3 : 2	300	200	1.1733	44.7	55.3
Blend 3 : 2	300	200	1.1967	45.5	54.5
8L 3 : 1	300	100	1.0963	61.6	38.4
8L 3 : 3	300	300	1.2412	29.8	70.2

the transition above T_g, which gives rise to the maximum, is designated as the Rouse modes by Ngai and coworkers and Huang and coworkers.[19–21] The loss peak of PVC at 36°C, which is corresponded to the glass transition temperature of plasticized PVC, indicates that the damping property of PVC is better than that of CIIR above room temperature.

As shown in Figure 3(b), the storage modulus (E') of CIIR and PVC are slightly different when the temperature is lower than −60°C. In the temperature range between −40°C and 40°C, the E' of CIIR decreases rapidly while the E' of PVC is slightly dropping. As a result, the E' of PVC is much larger than that of CIIR, especially at 20°C. Therefore, at the room temperature, CIIR/PVC multilayered composites fit well with the passive constrained layer damping characteristics, due to its soft-stiff alternating layer structure at room temperature. In the previous work,[22] it has been proved that the shear deformation and interface friction occur in multilayered composites, due to difference of the mechanical response between adjacent layers. The shear deformation and interface friction would convert more vibration energy into heat energy, which improves the damping property effectively.

Damping Properties

The damping properties of multilayered and conventional blended CIIR/PVC composites are displayed in Figure 4 and Table II. It can be observed that the loss peak of the CIIR/PVC multilayered damping composites is broadened with the layer number increasing. The 32-layer composite shows a wide effective damping temperature range from −32°C to 52°C ($\Delta T = 84$°C), which is much larger than that of 2-layer composite ($\Delta T = 48$°C) and conventional blended composite ($\Delta T = 28$°C). All of the multilayered damping composites have better damping property than conventional blend composite in the whole temperature range. The loss peak of CIIR is partially overlapped with that of PVC for the 8-layer and 32-layer composites, indicating that the effective damping area of the composites is broadened to the vicinity of room temperature, compared with that of neat CIIR. The 2-layer composite shows two tan δ peaks, which are corresponded to the glass transitions of CIIR and PVC, respectively, while the loss peak of Rouse modes relaxation disappears. The CIIR/PVC 2-layer composite is essentially a free-layer damping structure, due to the soft CIIR layer is not constrained by stiff PVC layer. As a result,

vibration energy is barely transferred into CIIR layer, hence CIIR layer is not cyclically shear deformed in such structure. Conversely, the maximum and the shoulder of CIIR are both suppressed in the conventional blended CIIR/PVC composite, but the maximum is suppressed to a higher extent, the maximum becomes lower than the shoulder, and even almost disappears, since PVC forms the continuous phase. The results suggest that multilayered damping structure is an effective way
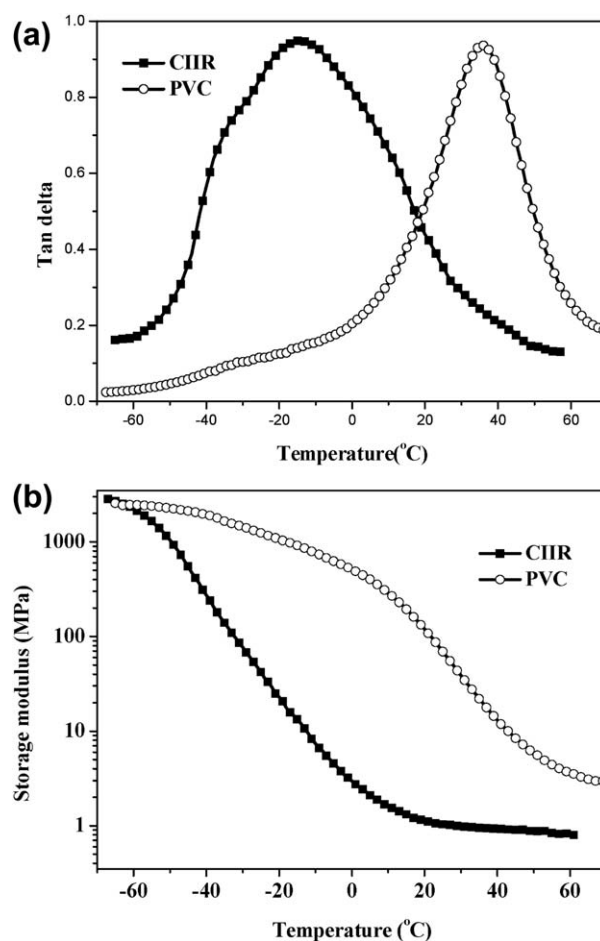

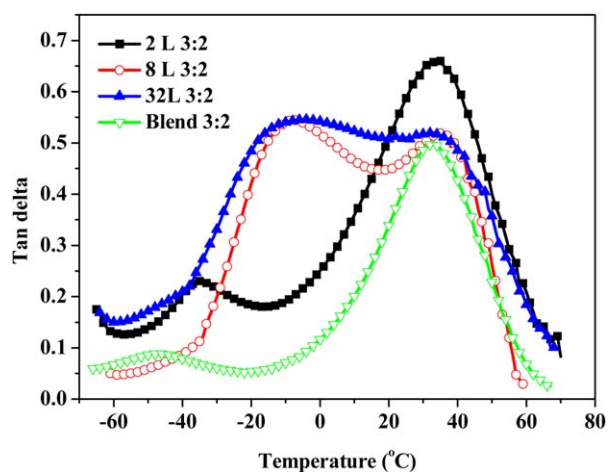**Figure 3.** Tan delta (a) and storage modulus and (b) versus temperature curves of PVC and CIIR.

Figure 4. Tan δ versus temperature curves of CIIR/PVC 2-layer, 8-layer, 32-layer, and conventional-blended composites. [Color figure can be viewed in the online issue, which is available at wileyonlinelibrary.com.]

for the damping property improvement, especially for broadening efficient damping temperature range.

To understand the molecular interactions between the CIIR and PVC layers, the interfacial adhesion strength is characterized by lap shear test. The interfacial adhesion strength, which is the maximal shear stress, can be obtained from Figure 5. It can be seen that interfacial adhesion strength is obviously improved the layer number increasing. The improvement of molecular interactions between the CIIR and PVC layers would promote the friction loss during the vibration field. This is also benefit to improve the damping property of the multilayered composites with the layer number increasing.

The temperature dependence of the tan δ for CIIR/PVC 8-layer damping composites with different extruding ratios is plotted in Figure 6. It can be observed that the loss peak of CIIR is partially overlapped with that of PVC for the three multilayered composites. Moreover, the tan δ value at high temperature (above 20°C) rises with increasing the PVC layer thickness, but the tan δ value at low temperature decreases. For the CIIR/PVC 8-layer damping composites with 3 : 1 extruding ratios, the loss peak at about 36°C is corresponded to the glass transition of

PVC, the loss peak at about −10°C is corresponded to the Rouse modes relaxation of CIIR, and the shoulder peak at about −45°C is corresponded to the glass transition of CIIR. It is interesting to note that, in the multilayered composites, the loss peak of the Rouse modes relaxation of CIIR moves to high temperature, compared with that of the neat CIIR (−15°C). One possible reason is that the Rouse modes relaxation of CIIR, which is long-scale and slow motion, is confined by the stiff PVC layers. Because the Rouse modes relaxation, which is the motion of longer chain segments requiring larger free volume, is sensitive to the change of the confinement. By contrast, the glass transition of CIIR is little affected, due to the motion segments is small (about several or tens nanometers).[23]

Flame-Retardant Properties

LOI test is one of the most useful tools to quantitatively evaluate flame-retardant property. The higher the LOI value, the better effective flame-retardant the material is. Generally, if the LOI value of an established material is less than 22, it should be associated to an inflammable material and higher than 27 means flame-retardant; while the plastic with an LOI value between 22 and 27 belongs to flammable material.[24] From LOI data, the CIIR has a LOI value of only 21 and is an easily flammable polymeric material, the PVC has a LOI value of 44 and is a flame-retardant polymeric material.

Figure 7 shows the effect of the layer number on the LOI values of CIIR/PVC multilayered composites. There are three different extruding ratios of CIIR and PVC layers. The LOI value of the 2-layer composite is less than 23, due to flammable CIIR layer is exposed to the air and can not be protected by the flame-retardant PVC layer aggressively. However, with the layer number increasing, the LOI value rises up obviously irrespective of the thickness ratio of CIIR and PVC layers. For example, the LOI value of the specimen with a extruding ratio of 3 : 2 approaches to about 36 when the layer number reaches 32, indicating that a transition from inflammable to flame-retardant state occurs. The LOI values of the 16-layer and 32-layer specimens with three different extruding ratios are larger than those of conventional blended composites with the same ratios. In the CIIR/PVC conventional blended composites, the fire may ignite the whole specimen due to the isotropic structure. While in the

Table II. The Damping Properties of PVC, CIIR, CIIR/PVC Multilayered, and Conventional Blend Composites

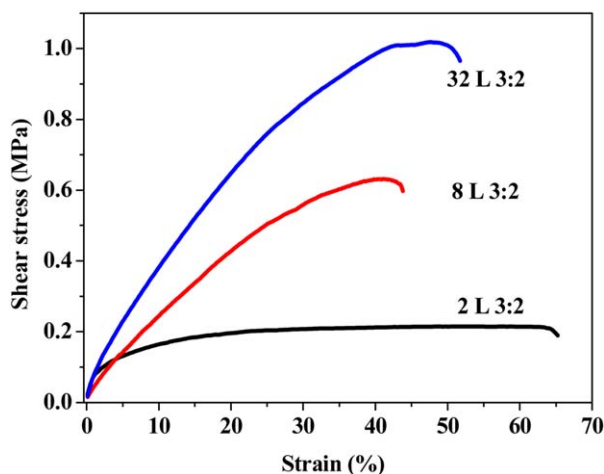| Sample code	Tan δ_{max}		Temperature range of Tan $\delta >0.3$		
	Value	T (°C)	T_1 (°C)	T_2 (°C)	ΔT (°C)
CIIR	0.95	−15	−47	28	75
PVC	0.94	36	9	57	48
2L 3 : 2	0.66	35	6	54	48
8L 3 : 2	0.54	−6	−25	50	75
32L 3 : 2	0.55	−5	−32	52	84
Blend 3 : 2	0.50	34	18	46	28
8L 3 : 1	0.57	−3	−47	48	95
8L 3 : 3	0.54	31	−22	46	68

Figure 5. The interfacial shear stress–strain curves of CIIR/PVC multilayered composites. [Color figure can be viewed in the online issue, which is available at wileyonlinelibrary.com.]

CIIR/PVC multilayered composites, the CIIR and PVC layers are distributed alternately vertical to the burning direction, and PVC layers act as insulating barriers, which is flame-retardant at lower oxygen saturation than its LOI. According to the literature,[14] the confined burning space can effectively retard the combustion of the material, and the layer interfaces in the multilayered system is considered to play a crucial role in retarding the spread of fire, because less surface area of CIIR contacting oxygen results in the increase of the LOI value.

As shown in Figure 8(a,b), the thermal decomposition of PVC is divided into two stages: the thermal decomposition in the first stage is mainly the evolution of hydrogen chloride. The thermal decomposition in the second stage is mainly the cyclization of conjugated polyene sequences to form aromatic compounds.[11] The evolved hydrogen chloride and the aromatic compounds act as an insulating barrier to reduce heat and fuel transfer between the heat source and the polymer during the burning. However, the layer number has little effect on the
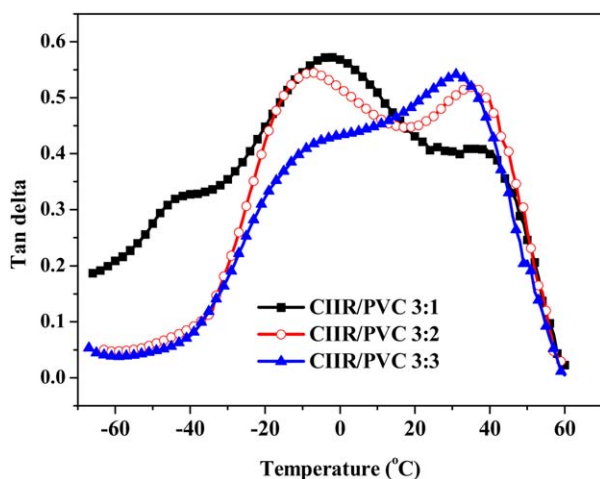

Figure 7. The LOI of PVC/CIIR multilayered composites with different extruding ratios, the LOI of PVC/CIIR conventional blended composites with 3 : 1, 3 : 2, and 3 : 3 ratios are shown as the solid straight line, dash straight line, and dash-dot straight line, respectively. [Color figure can be viewed in the online issue, which is available at wileyonlinelibrary.com.]

Figure 6. Tan δ versus temperature curves of CIIR/PVC 8-layer composites with different extruding ratios. [Color figure can be viewed in the online issue, which is available at wileyonlinelibrary.com.]
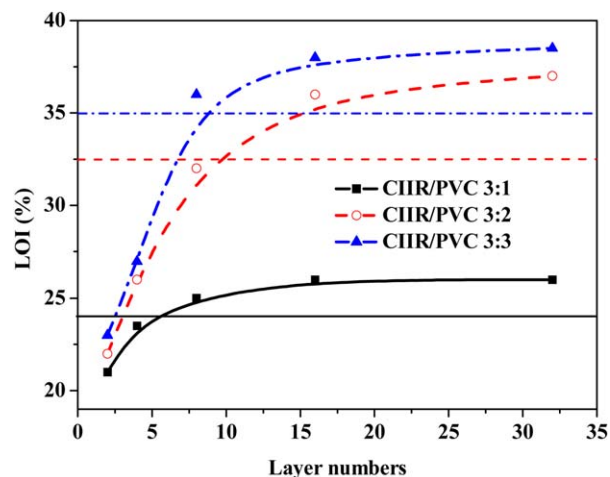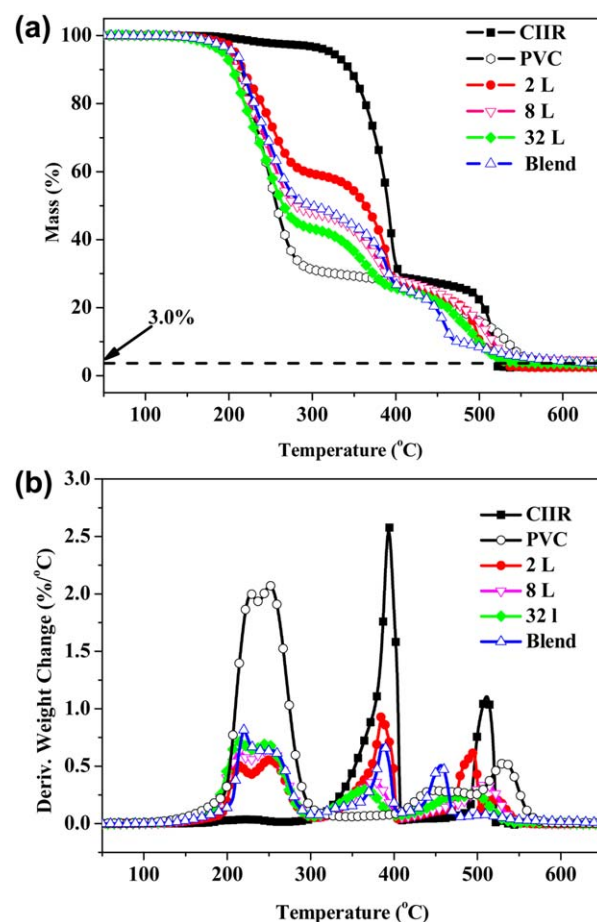
Figure 8. TGA (a) and DTG (b) curves for CIIR, PVC, CIIR/PVC multilayered, and conventional-blended composites with the extruding ratio of 3:2. [Color figure can be viewed in the online issue, which is available at wileyonlinelibrary.com.]
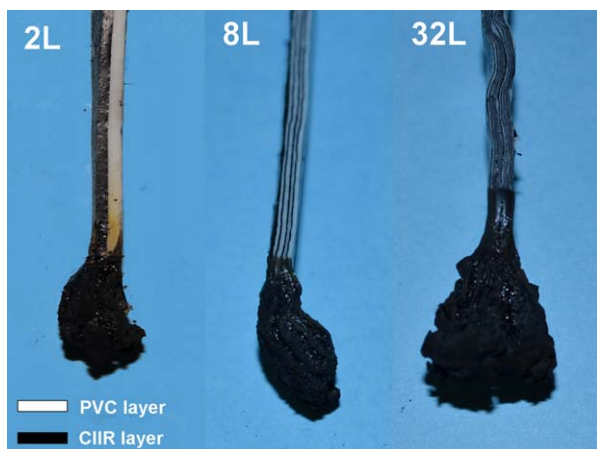
Figure 9. The digital images of char residual for 2-layer (a), 8-layer (b), and 32-layer CIIR/PVC composites. [Color figure can be viewed in the online issue, which is available at wileyonlinelibrary.com.]

amount of char residue, since the residues of multilayered and conventional blended CIIR/PVC composites are almost around 3.0% [Figure 8(a)]. Hence, the amount of char residue is not the main reason for the improvement of the flame-retardant property. In addition, Figure 9 exhibits the digital pictures of the charred residues of the multilayered composites. The interfacial delamination is not observed during the burning process, and the multilayered structure still exists in the char residue. The char layer acts as an insulating barrier to reduce heat and fuel transfer between the heat source and the specimen.

It is worth noting that thermal stability of PVC layer decreases with increasing the layer number in the first TGA stage. The reason for this phenomenon is that the thermal decomposition of PVC layer, which occurs first at the continuous interfaces, is accelerated with increasing the layer number. The TGA curve of 8-layer composite is similar to that of conventional blended composite, resulting in slight distinction of the LOI value (Figure 7). With increasing the layer number, the TGA curves of multilayered composites approach to that of neat PVC, thus the LOI increases and multilayered composites are inflammable to flame-retardant.

CONCLUSION

In conclusion, the CIIR/PVC multilayered damping composites have better damping and flame-retardant properties than conventional blended composites. The effective damping temperature range is broadened with the layer number increasing, and the damping property at high temperature (above 20°C) is significantly improved. The tan δ at different temperatures can also be adjusted by changing the extruding ratio of the CIIR layer and PVC layer. With increasing the layer number, the LOI of the multilayered composites are increased. This work provides a new thought for manufacturing flame-retarding composites with excellent damping properties through multilayered coextrusion.

ACKNOWLEDGMENTS

REFERENCES

 1. Mao, X. D.; Xu, S. A.; Wu, C. F. *Polym. Plast. Technol.* **2008**, *47*, 209.

 2. Li, C.; Wu, G. Z.; Xiao, F. Y.; Wu, C. F. *J. Appl. Polym. Sci.* **2007**, *106*, 2472.

 3. Qu, L. L.; Huang, G. S.; Wu, J. R.; Tang, Z. H. *J. Mater. Sci.* **2007**, *42*, 7256.

 4. Su, C.; He, P.; Yan, R. J.; Zhao, C. B. *Polym. Compos.* **2012**, *33*, 860.

 5. Li, C.; Xu, S. A.; Xiao, F. Y.; Wu, C. F. *Eur. Polym. J.* **2006**, *42*, 2507.

 6. Liao, F. S.; Su, A. C.; Hsu, T. C. *Polymer* **1994**, *35*, 2579.

 7. Lu, S. Y.; Hamerton, I. *Prog. Polym. Sci.* **2002**, *27*, 1661.

 8. Zhang, F. S.; He, G. S.; Xu, K. M.; Wu, H.; Guo, S. Y.; Zhang, C. L. *J. Appl. Polym. Sci.* **2014**, *131*, 40464.

 9. Wu, J. R.; Huang, G. S.; Wang, X. A.; He, X. J.; Lei, H. X. *J. Polym. Res.* **2011**, *18*, 2213.

10. Li, M. J.; Cheng, Y.; Xu, Y. W.; Qin, Y.C. *J. Appl. Polym. Sci.* **2013**, *129*, 1334.

11. Xiang, P.; Zhao, X. Y.; Xiao, D. L.; Lu, Y. L.; Zhang, L. Q. *J. Appl. Polym. Sci.* **2008**, *109*, 106.

12. Pi, H.; Guo, S. Y.; Ning, Y. *J. Appl. Polym. Sci.* **2003**, *89*, 753.

13. Yamada, N.; Shoji, S.; Sasaki, H.; Nagatani, A.; Yamaguchi, K.; Kohjiya, S.; Hashim, A. S. *J. Appl. Polym. Sci.* **1999**, *71*, 855.

14. Chen, B. S.; Gao, W. L.; Shen, J. B.; Guo, S. Y. *Compos. Sci. Technol.* **2014**.

15. Shen, J. B.; Li, J.; Guo, S. Y. *Polymer* **2012**, *53*, 2519.

16. Shen, J. B.; Wang, M.; Li, J.; Guo, S. Y.; Xu, S. X.; Zhang, Y. Q. *Eur. Polym. J.* **2009**, *45*, 3269.

17. Xu, S.; Wen, M.; Li, J.; Guo, S. Y.; Wang, M.; Du, Q. *Polymer* **2008**, *49*, 4861.

18. Fitzgerald, E. R.; Grandine, L. D.; Ferry, J. D. *J. Appl. Phys.* **1953**, *24*, 650.

19. Rizos, A. K.; Ngai, K. L.; Plazek, D. J. *Polymer* **1997**, *38*, 6103.

20. Plazek, D. J.; Chay, I. C.; Ngai, K. L.; Roland, C. M. *Macromolecules* **1995**, *28*, 6432.

21. Wu, J. R.; Huang, G. S.; Wang, X. A.; He, X. J.; Zheng, J. *Soft Matter* **2011**, *7*, 9224.

22. Zhang, F. S.; Guo, M. L.; Xu, K. M.; He, G. S.; Wu, H.; Guo, S. Y. *Compos. Sci. Technol.* **2014**, *101*, 167.

23. Wu, J. R.; Huang, G. S., Wang, X. A., He, X. J., Lei, H. X. *J. Polym. Sci. Pol. Phys.* **2010**, *48*, 2165.

24. Gao, L. P.; Wang, D. Y.; Wang, Y. Z.; Wang, J. S.; Yang, B. *Polym. Degrad. Stabil.* **2008**, *93*, 1308.